Inorg. Chem. **2009**, *48*, 854−860

Co^{II} Molecular Square with Single-Molecule Magnet Properties

Dayu Wu,[†,§] Dong Guo,[†] You Song,[†] Wei Huang,[†] Chunying Duan,*[,†] Qingjin Meng,[†] and Osamu Sato[‡]

State Key Laboratory of Coordination Chemistry, Nanjing University, Nanjing 210093, China, and Institute for Materials Chemistry and Engineering, Kyushu University, 6-1 Kasuga, 816-8580 Fukuoka, Japan

Received July 2, 2008

A new tetranuclear cobalt(II) molecular square in which adjacent Co^{II} centers are linked by a μ_2-bridging oxygen atom and a N−N bridge along the edges of the square has been designed for single-molecule magnets (SMMs) with high anisotropy barriers. The overall intramolecular ferromagnetic coupling at low temperature combined with the slow relaxation at static zero fields suggests a SMM behavior for this molecular square. The zero-field cooled magnetization (ZFCM) and field cooling magnetization (FCM) at 10 Oe illustrate the nonreversibility and bifurcation below 4.5 K. The deviations of magnetization from the saturated value in strong applied fields demonstrate the participation of low-lying excited states. The peaks of the out-of-phase signals are observed corresponding to coincidence of the applied ac field oscillation frequency with the relaxation rate.

Introduction

Single-molecule magnets (SMMs) that possess slowly relaxing magnetic moments offer an intercross between molecule-based ferromagnets and nanoscale magnetic materials because each individual monodisperse molecular entity of SMMs exhibits a unique concomitance of both macroscopic and quantum regime properties.[1,2] SMMs, combining the advantages of the molecular scale with the properties of bulk magnetic materials, become very attractive for high-density information storage and also, because of their long coherence times,[3] for quantum computing.[4] Moreover, their molecular nature leads to appealing quantum effects of the static and dynamic magnetic properties.[5,6] The rich physics behind the magnetic behavior produces interesting effects such as negative differential conductance and complete current suppression,[7,8] which could be used in molecular spintronics.[9]

To understand the correlation between the structure and magnetic properties of these molecules, the synthetic strategies have been extensively investigated with the rapidly growing family of SMMs, and the SMM behaviors have been observed in a variety of metal complexes.[10−14] The ongoing research for SMMs with high anisotropy barriers (preferen-

* To whom correspondence should be addressed. E-mail: cyduan@dlut.edu.cn.

† Nanjing University.

§ Current address: Anhui Key Laboratory of Functional Coordination Chemistry, School of Chemistry and Chemical Engineering, Anqing Normal University, 246011, Anqing, China.

‡ Kyushu University.

(1) (a) Christou, G.; Gatteschi, D.; Hendrickson, D. N.; Sessoli, R. *Mater. Res. Soc. Bull.* **2000**, *25*, 66–71. (b) Gatteschi, D.; Sessoli, R.; Villain, J. *Molecular Nanomagnets*; Oxford University Press: New York, 2007.

(2) (a) Wernsdorfer, W.; Allaga-Alcalde, N.; Hendrickson, D. N.; Chritou, G. *Nature* **2002**, *416*, 406–409. (b) Coronado, E.; Palacio, F.; Veciana, J. *Angew. Chem., Int. Ed.* **2003**, *42*, 2570–2572.

(3) (a) Carretta, S.; Santini, P.; Amoretti, G.; Guidi, T.; Copley, J. R. D.; Qiu, Y.; Caciuffo, R.; Timco, G.; Winpenny, R. E. P. *Phys. Rev. Lett.* **2007**, *98*, 167401. (b) Ardavan, A.; Rival, O.; Morton, J. J. L.; Blundell, S. J.; Tyryshkin, A. M.; Timco, G. A.; Winpenny, R. E. P. *Phys. Rev. Lett.* **2007**, *98*, 057201.

(4) (a) Leuenberger, M. N.; Loss, D. *Nature* **2001**, *410*, 789–793. (b) Troiani, F.; Ghirri, A.; Affronte, M.; Carretta, S.; Santini, P.; Amoretti, G.; Piligkos, S.; Timco, G.; Winpenny, R. E. P. *Phys. Rev. Lett.* **2005**, *94*, 207208. (c) Lehmann, J.; Gaita-Arino, A.; Coronado, E.; Loss, D. *Nature Nanotech.* **2007**, *2*, 312–317.

(5) Thomas, L.; Lionti, F.; Ballou, R.; Gatteschi, D.; Sessoli, R.; Barbara, B. *Nature* **1996**, *383*, 145–147.

(6) (a) Friedman, J. R.; Sarachik, M. P.; Tejada, J.; Ziolo, R. *Phys. Rev. Lett.* **1996**, *76*, 3830–3833. (b) Wernsdorfer, W.; Sessoli, R. *Science* **1999**, *284*, 133–135.

(7) Heersche, H. B.; de Groot, Z.; Folk, J. A.; van der Zant, H. S. J.; Romeike, C.; Wegewijs, M. R.; Zobbi, L.; Barreca, D.; Tondello, E.; Cornia, A. *Phys. Rev. Lett.* **2006**, *96*, 206801.

(8) Jo, M. H.; Grose, J. E.; Baheti, K.; Deshmukh, M. M.; Sokol, J. J.; Rumberger, E. M.; Hendrickson, D. N.; Long, J. R.; Park, H.; Ralph, D. C. *Nano. Lett.* **2006**, *6*, 2014–2020.

(9) Bogani, L.; Wernsdorfer, W. *Nat. Mater.* **2008**, *7*, 179–186.

(10) Soler, M.; Wernsdorfer, W.; Folting, K.; Pink, M.; Christou, G. *J. Am. Chem. Soc.* **2004**, *126*, 2156–2165.

(11) Oshio, H.; Hoshino, N.; Ito, T.; Nakano, M. *J. Am. Chem. Soc.* **2004**, *126*, 8805–8812.

(12) Ishikawa, N.; Sugita, M.; Wernsdorfer, W. *J. Am. Chem. Soc.* **2005**, *127*, 3650–3651.

10.1021/ic8012188 CCC: $40.75
Published on Web 01/07/2009

Scheme 1

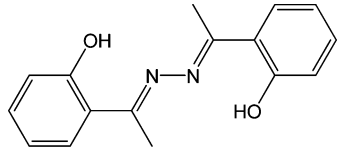

H_2L

tially above room temperature to overcome the thermal fluctuation) is driving the increasing interest in the magnetic properties of spin-bearing metal ion arrays. As a result of its large anisotropy, Co(II) might be a good candidate ion for SMMs because the strong Ising-type anisotropic contribution of Co(II) has been demonstrated in several single-chain magnets (SCMs).[15−17] Recently, Hendrickson and coworkers reported a tetranuclear cage as the first example of Co-based SMMs.[18] Murrie et al. reported the second Co-based SMM of a hexanuclear cagelike complex.[19] Unfortunately, both examples revealed the difficulties in the indication that these cobalt architectures are SMMs because of the ambiguous features for characteristic SMMs. To obtain the Co-based SMMs, several groups have exploited a number of synthetic strategies that show some interesting results.[20−24] Lehn's group showed that the Co^{II}_4 entity could represent an isolated magnetic domain, a model system for studying magnetic interactions in discrete entities.[25] Herein we report a new Co^{II}-based molecular square, Co_4L_4, in which the ligand L^{2-} is the deprotonated *N*,*N*′-di[1-(2-hydroxyphenyl)ethlidene]hydrazone (Scheme 1). The overall intramolecular ferromagnetic coupling at low temperature combined with the slow relaxation at static zero fields suggests its SMM behavior.

Experimental Section

All chemicals used were of reagent grade or better and were obtained from commercial sources and used without further purification. The ligand H_2L, *N*,*N*′-di[1-(2-hydroxyphenyl)ethlidene]-hydrazone, was prepared according to the literature method.[26] Elemental analyses (C, H, and N) were carried out on a Perkin-Elmer 240 analyzer. IR spectra were recorded using KBr pellets on a Vector 22 Bruker spectrophotometer in the 4000−400 cm^{-1} region. Solid UV−vis spectra were obtained on a Shimadzu 3100 spectrophotometer at room temperature.

Preparation of the Compound $Co_4L_4 \cdot 0.5H_2O$ (1). A CH_3OH solution containing H_2L (0.1 mmol, 0.027 g) and NaOH (0.2 mmol, 0.008 g) was refluxed for 30 min prior to the addition of 10 mL of CH_3OH solution of $Co(ClO_4)_2 \cdot 6H_2O$ (0.1 mmol, 0.037 g) under a N_2 atmosphere. The resulting solution was stirred for another 30 min at the boiling point, followed by cooling at room temperature to form a precipitate. The orange powder was filtered and dried over P_2O_5 under vacuum. We obtained the crystals suitable for X-ray diffraction by evaporating the filtrate after 1 week, which was characterized to be the same with the powder using spectroscopic characterization, powder X-ray diffraction, and element analysis. Anal. Calcd for $C_{64}H_{56}N_8O_8Co_4 \cdot 0.5H_2O$: C, 58.66; H, 4.39; N 8.56. Found: C, 58.74; H, 4.89; N, 8.34. IR (solid KBr pellet, cm^{-1}): 3447.5 (m), 1600.9 (s), 1567.3 (m), 1525.6 (m), 1439.4 (s), 1338.2 (s), 1236.8 (s), 1111.5 (m), 859.6 (w), 748.8 (m), 679.1 (w), 627.8 (w), 579.9 (w). UV−vis spectra λ, nm: 442.

Crystallography. Intensity data of compound **1** were collected on a Siemens SMART-CCD diffractometer with graphite-monochromated Mo Kα ($\lambda = 0.71073$ Å) using the SMART and SAINT programs.[27] Data (45 frames) were collected at 298 K with an oscillation range of 1 deg/frame and an exposure time of 15 s/frame. Indexing and unit cell refinement were based on all observed reflections from those 45 frames. The structure was solved by direct methods and refined on F^2 by full-matrix least-squares methods with SHELXTL version 5.1.[28] Non-hydrogen atoms were anisotropically refined, except for the disordered solvent molecules. Hydrogen atoms were geometrically fixed and refined by the use of a riding model. Crystal data for **1** ($C_{64}H_{56}N_8O_8Co_4 \cdot 0.5H_2O$): $M_r = 1309.09$; monoclinic; space group: $P2_1/c$; $a = 15.595(2)$ Å, $b = 16.304(2)$ Å, $c = 25.064(3)$ Å; $\beta = 103.38(1)°$; $V = 6199.8(11)$ $Å^3$; $Z = 4$; $D_c = 1.403$ g/cm^3; $T = 293(2)$ K. A total of 30 450 reflections were processed to give 10 907 unique reflections ($R_{int} = 0.070$). Refinement converged to $R = 0.052$, $wR(F^2) = 0.069$, and $S = 1.025$ for 5942 reflections with $I > 2\sigma(I)$, and $R = 0.111$, $wR(F^2) = 0.075$, and $S = 1.031$ for 10 907 unique reflections and 761 parameters (CCDC-616883).

Magnetic Measurements. Magnetic susceptibility measurements were obtained with the use of a Quantum Design MPMS-XL7 SQUID magnetometer at temperatures ranging from 1.8 to 300 K. The dc measurements were performed using applied fields in the range of 0.05−7 T. The settle mode was employed for ZFC−FC measurements. Hysteresis loops were determined according to the following method by Gatteschi and coworkers,[29] which fixed the characteristic time windows of the measurements: When a measurement at a given field has ended, the field is changed during 10 s to reach the next value. After a pause of 30 s, to allow stabilization, the measurements at the new value of applied field are taken. The

(13) Osa, S.; Kido, T.; Matsumoto, N.; Re, N.; Ochaba, A.; Mrozinski, J. *J. Am. Chem. Soc.* **2004**, *126*, 420–421.
(14) Wang, C. F.; Zuo, J. L.; Bartlet, B. M.; Song, Y.; Long, J. R.; You, X. Z. *J. Am. Chem. Soc.* **2006**, *128*, 7162–7163.
(15) Liu, T. F.; Fu, D.; Gao, S.; Zhang, Y. Z.; Sun, H. L.; Liu, Y. *J. Am. Chem. Soc.* **2003**, *125*, 13976–13977.
(16) Pardo, E.; Ruiz-Garcia, R.; Lloret, F.; Faus, J.; Julve, M.; Journaux, Y.; Delgado, F.; Ruiz-Peres, C. *Adv. Mater.* **2004**, *16*, 1597–1600.
(17) Zheng, Y. Z.; Tong, M. L.; Zhang, W.-X.; Chen, X. M. *Angew. Chem., Int. Ed.* **2006**, *45*, 6310–6314.
(18) Yang, E. C.; Hendrickson, D. N.; Wernsdorfer, W.; Nakano, M.; Zakharov, L. N.; Sommer, R. D.; Rheingold, A. L.; Ledezma-Gairaud, M.; Christou, G. *J. Appl. Phys.* **2002**, *91*, 7382–7384.
(19) Murrie, M.; Teat, S. J.; Stoeckli-Evans, H.; Güdel, H. U. *Angew. Chem., Int. Ed.* **2003**, *42*, 4653–4656.
(20) Moragues-Canovas, M.; Talbot-Eeckelaers, C. E.; Catala, L.; Lloret, F.; Wernsdorfer, W.; Brechin, E. K.; Mallah, T. *Inorg. Chem.* **2006**, *45*, 7038–7040.
(21) Zhang, Y. Z.; Wernsdorfer, W.; Pan, F.; Wang, Z.-M.; Gao, S. *Chem. Commun.* **2006**, 3302–3304.
(22) Ferguson, A.; Parkin, A.; Sanchez-Benitez, J.; Kamenev, K.; Wernsdorfe, W.; Murrie, M. *Chem. Commun.* **2007**, 3473–3475.
(23) Schelter, E. J.; Karadas, F.; Avendano, C.; Prosvirin, A. V.; Wernsdorfer, W.; Dunbar, K. R. *J. Am. Chem. Soc.* **2007**, *127*, 8139–8149.
(24) Zeng, M. H.; Yao, M. X.; Liang, H.; Zhang, W. X.; Chen, X. M. *Angew. Chem., Int. Ed.* **2007**, *46*, 1832–1835.
(25) Waldmann, O.; Ruben, M.; Ziener, U.; Mu1ller, P.; Lehn, J. M. *Inorg. Chem.* **2006**, *45*, 6535–6540.
(26) Gunther, L.; Kurt, S. *Ber. Dtsch. Chem. Ges. B* **1944**, *77*, 293–296.
(27) *SMART and SAINT: Area Detector Control and Integration Software*; Siemens Analytical X-ray Systems, Inc.: Madison, WI, 1996.
(28) *SHELXTL V5.1, Software Reference Manual*; Bruker, AXS, Inc.: Madison, WI, 1997.
(29) The measurement methods for the hysteresis loops were similar to that by D. Gatteschi and coworkers in ref 5, which fixed the characteristic time windows of the measurements: When a measurement at a given field has ended, the field is changed during 10 s to reach the next value. After a pause of 30 s, to allow stabilization, the measurements at the new value of applied field are taken. The field increment is fixed at 0.02 T between 1.5 and −1.5 kOe.

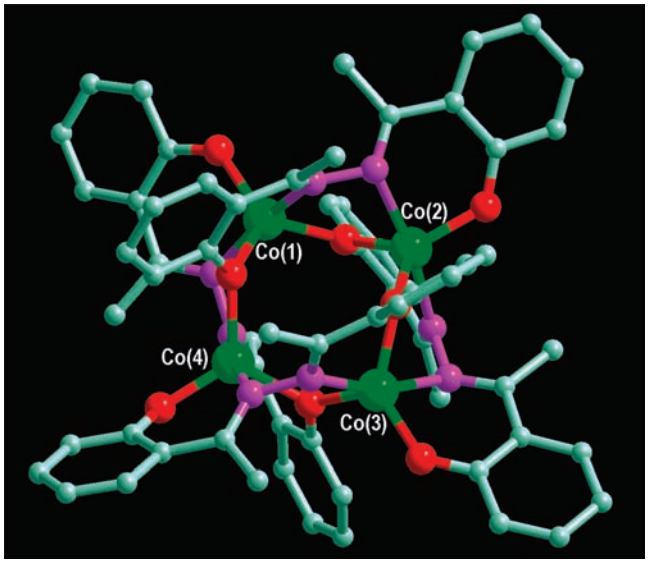

Figure 1. Structure of the tetranuclear molecular square Co_4L_4. The cobalt, oxygen, nitrogen, and carbon atoms are emphasized in green, red, magenta, and cyan, respectively.

magnetization variations from 1500 to −1500 Oe were observed with a field increment fixed at 0.02 T.

Results and Discussion

Structure Description of Complex 1. Compound **1** ($Co_4L_4 \cdot 0.5H_2O$) crystallized in a $P2_1/c$ space group with an asymmetric unit containing a neutral tetranuclear molecular square Co_4L_4 (Figure 1) and a half-water molecule. Each Co^{II} center in the Co_4L_4 fragment adopted a penta-coordination geometry. The topological parameters,[30] τ, defined as $\tau = [(\theta - \varphi)/60]100$ were calculated as 0.74(9) for Co(1) to 0.81(8) for Co(4). The parameter τ was 100% if the coordination geometry was purely trigonal bipyramidal, whereas τ was 0% if the geometry was purely square pyramidal. Thus, the coordination geometry for exchange cobalt was considered to be slightly distorted trigonal bipyramidal geometry, where the equatorial plane was formed by one terminal oxygen atom and two μ_2-bridged oxygen atoms, whereas the axial positions were sited by two hydrazine nitrogen atoms. The intracluster Co···Co separations were about 3.38 Å along the edges of the square, whereas the diagonal Co···Co separations were about 4.75 Å. Adjacent Co^{II} centers were linked by a μ_2-bridging oxygen atom and a N−N bridge along the edges of the square with the Co−O−Co angle and the Co−N−N−Co torsion angle being 115 and 50°, respectively. Such a specific bridging mode not only induces four Co^{II} centers to exhibit the same chirality but also could provide an opportunity to obtain interesting magnetic properties.[31,32] The Co−O bond distances of terminal oxygen atoms ranged from 1.898(3) to 1.913(3) Å, whereas, the Co−O bond distances of the μ_2-bridged oxygen atoms ranged from 1.971(3) to 1.995(3)Å, respectively (Table 1). No significant intermolecular interaction could be found in its solid packing because the shortest intermolecular atom···atom separation was ca. 3.48 Å, and the neutral complex was hydrophobic to exclude the formation of efficient hydrogen bonds. The shortest intermolecular Co···Co separation of ca. 8.80 Å suggests that the intermolecular spin-exchange coupling should be very weak or negligible.

Table 1. Selected Bond Distances (Å) and Angles (deg) around Co(II) Ions

Co(1)−O(3)	1.902(3)	Co(1)−O(3)	1.971(3)
Co(1)−O(7)	1.988(3)	Co(1)−N(3)	2.109(4)
Co(1)−N(7)	2.147(4)	Co(3)−O(5)	1.913(3)
Co(3)−O(1)	1.979(3)	Co(3)−O(4)	1.995(3)
Co(3)−N(5)	2.094(4)	Co(3)−N(1)	2.133(4)
Co(2)−O(2)	1.906(3)	Co(2)−O(7)	1.989(3)
Co(2)−O(4)	1.994(3)	Co(2)−N(2)	2.083(3)
Co(2)−N(4)	2.104(3)	Co(4)−O(8)	1.898(3)
Co(4)−O(1)	1.981(3)	Co(4)−O(6)	1.987(3)
Co(4)−N(8)	2.079(3)	Co(4)−N(6)	2.097(3)
O(1)−C(1)	1.358(5)	O(2)−C(16)	1.305(5)
O(3)−C(17)	1.300(5)	O(4)−C(32)	1.335(4)
O(5)−C(33)	1.325(5)	O(6)−C(48)	1.333(4)
O(7)−C(49)	1.347(4)	O(8)−C(64)	1.316(6)
O(3)−Co(1)−O(6)	119.7(1)	O(2)−Co(2)−O(7)	122.4(1)
O(3)−Co(1)−O(7)	125.0(1)	O(2)−Co(2)−O(4)	120.1(1)
O(6)−Co(1)−O(7)	115.3(1)	O(7)−Co(2)−O(4)	117.5(1)
O(3)−Co(1)−N(3)	86.9(1)	O(2)−Co(2)−N(2)	89.1(1)
O(6)−Co(1)−N(3)	99.7(1)	O(7)−Co(2)−N(2)	98.3(1)
O(7)−Co(1)−N(3)	82.4(1)	O(4)−Co(2)−N(2)	83.8(1)
O(3)−Co(1)−N(7)	102.2(1)	O(2)−Co(2)−N(4)	98.1(1)
O(6)−Co(1)−N(7)	86.7(1)	O(7)−Co(2)−N(4)	86.3(1)
O(7)−Co(1)−N(7)	82.2(1)	O(4)−Co(2)−N(4)	84.0(1)
N(3)−Co(1)−N(7)	164.6(1)	N(2)−Co(2)−N(4)	167.8(1)
O(5)−Co(3)−O(1)	119.8(1)	O(8)−Co(4)−O(1)	120.4(1)
O(5)−Co(3)−O(4)	122.9(1)	O(8)−Co(4)−O(6)	119.0(1)
O(1)−Co(3)−O(4)	117.4(1)	O(1)−Co(4)−O(6)	120.4(1)
O(5)−Co(3)−N(5)	89.0(1)	O(8)−Co(4)−N(8)	91.0(2)
O(1)−Co(3)−N(5)	83.4(1)	O(1)−Co(4)−N(8)	97.1(1)
O(4)−Co(3)−N(5)	96.5(1)	O(6)−Co(4)−N(8)	85.2(1)
O(5)−Co(3)−N(1)	100.9(1)	O(8)−Co(4)−N(6)	96.2(1)
O(1)−Co(3)−N(1)	83.0(1)	O(1)−Co(4)−N(6)	86.2(1)
O(4)−Co(3)−N(1)	86.6(1)	O(6)−Co(4)−N(6)	84.2(1)
N(5)−Co(3)−N(1)	166.0(1)	N(8)−Co(4)−N(6)	169.2(2)

Direct Current Magnetic Susceptibility Studies. Being identified by XRD as a pure phase (Figure S1 in the Supporting Information), polycrystalline powder of compound **1** was used for variable-temperature magnetic susceptibility studies at the relatively weak dc applied field (100 Oe). Upon cooling from room temperature, the value of $\chi_M T$ showed a continuous decrease from a value of 8.3 emu·K·mol^{-1} (Figure 2a), corresponding to four noninteracting $S_i = 3/2$ centers with a g factor of 2.1, to a rounded minimum of 5.2 emu·K·mol^{-1} at 26 K. Below this temperature, $\chi_M T$ increased dramatically and reached an abrupt maximum at ca. 4 K. The decrease in $\chi_M T$ down to 26 K basically corresponded to a single-ion behavior.[33] The magnetic behavior in the high-temperature region can be explained if we bear in mind that the high-spin Co(II) in trigonal bipyramidal symmetry (D_{3h}) has an orbitally non-

(30) In pentacoordinated systems, the actual geometry of the complex can be described by a structural index parameter τ such that $\tau = (\beta-\alpha)/60°$, where β and α are the two largest angles ($\beta > \alpha$). See the details: Addison, A. W.; Rao, T. N.; Reedijk, J.; Rijn, J.; Verschoor, G. C. *J. Chem. Soc., Dalton Trans.* **1984**, 1349–1355.

(31) Grove, H.; Kelly, T. L.; Thompson, L. K.; Zhao, L.; Xu, Z.; Abedin, T. S. M.; Miller, D. O.; Goeta, A.; Wilson, E. C.; Howard, J. A. K. *Inorg. Chem.* **2004**, *43*, 4278–4288.

(32) Parsons, S. R.; Thompson, L. K.; Dey, S. K.; Wilson, C.; Howard, J. A. K. *Inorg. Chem.* **2006**, *45*, 8832–8834.

(33) (a) Herchel, R.; Boča, R. *Dalton Trans.* **2005**, 1352–1353. (b) Marshall, S. R.; Rheingold, A. L.; Dawe, L. N.; Shum, W. W.; Kitamura, C.; Miller, J. S. *Inorg. Chem.* **2002**, *41*, 3599–3601.

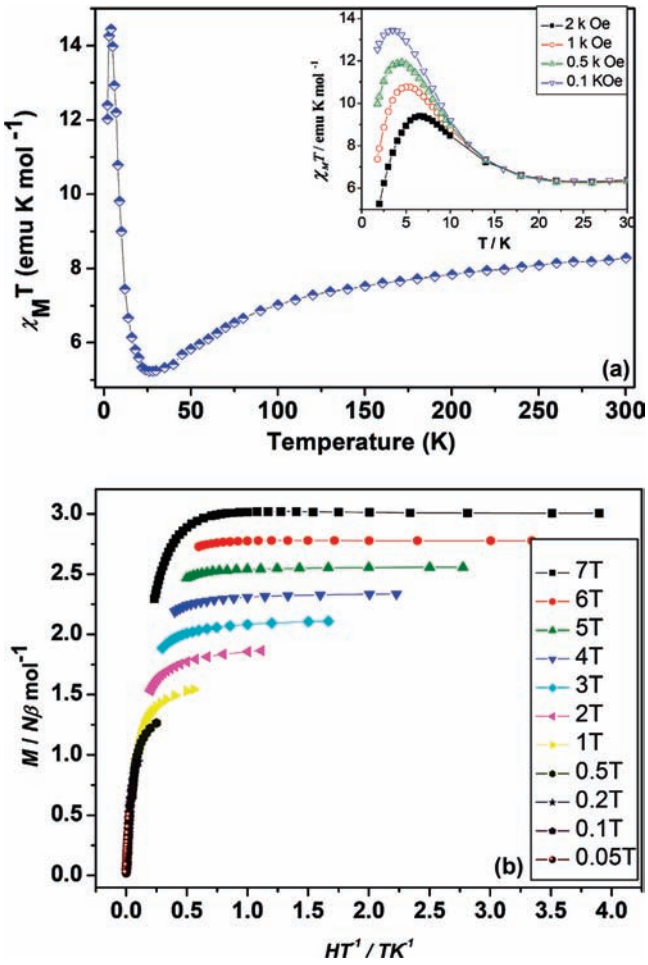

Figure 2. (a) Temperature dependence of $\chi_M T$ in an applied field of 100 Oe. The insert exhibits the temperature dependence of $\chi_M T$ in different applied field. The data at 0.1, 0.5, 1, and 2 KOe are drawn in blue, green, red, and black, respectively. (b) Plot of reduced magnetization measurement of randomly oriented powder in the temperature range from 2 to 10 K. The lines are guided for view.

degenerate ground state ($^4A_2'$), which could be split into two Kramers doublets because of geometrical distortion.[34−39] However, the observed increase in $\chi_M T$ below this temperature is no longer coming from the single-ion behavior but rather from a ferromagnetic $Co^{II}-Co^{II}$ exchange interaction. A similar magnetic behavior has been observed in a mononuclear cobalt(II) complex with trigonal bipyramidal symmetry, where the abrupt increase in the low-temperature region was seen as the evidence of a magnetic ordering.[33a] In our case, either magnetic ordering or ferromagnetic exchange coupling is possible. Treated as a ferromagnetic exchange coupling case, the maximum $\chi_M T$ value (14.44 emu K mol^{-1}) at ca. 4.0 K corresponds well to the four effective $S' = 1/2$ states, each with a g' value of 4.3 interacting in a ferromagnetic manner. The large g' value might reflect an admixture of the upper excited state $^4E''$ with the ground state $^4A_2'$, which may bring the orbital angular momentum into the ground term[34,38,39] because when the structure is distorted and the symmetry deviates from ideal D_{3h}, the orbital momentum quenching of the ground $^4A_2'$ term may not be sufficient.

The field-dependent magnetizations in strong applied fields (1−7 T) at 1.8−10 K reveal that the isofield lines are far from superposition (Figure 2b); the deviations of magnetization from the saturated value demonstrate the participation of low-lying excited states in strong applied fields. The fact that the mean susceptibility below 15 K strongly depends on the magnetic field (insert of Figure 2a) also suggests the very close levels and crossing of the levels when a magnetic field is applied.[40,41] To exclude the participation of low-lying excited states and ensure a well-isolated magnetic ground state,[42] the field-dependent magnetizations in weak fields (0.05−0.5 T) were also measured, suggesting the presence of magnetic anisotropy in the current system. However, the attempts to fit the magnetic susceptibility below 26 K using an anisotropic exchange Hamiltonian were unsuccessful because of the large number of adjustable parameters and the invalidation of the van Vleck equation here, assuming linear magnetic behavior.[30,41]

The accurate measurements[43] at 1.8 K show the presence of a hysteretic loop with a coercive field of 105 Oe and a remnant magnetization of 0.096 $N\beta \cdot mol^{-1}$. The coercivities of the hysteresis loops rapidly increase with the decrease in temperature in the range of 4.2−1.8 K (Figure 3a). These results suggest a magnet-type behavior. The temperature dependence and area within the hysteresis loops indicate that the molecule has considerable negative magnetic anisotropy, as expected for an SMM. The zero-field cooled magnetization (ZFCM) and field cooling magnetization (FCM) at 10 Oe illustrate the nonreversibility and bifurcation below 4.5 K (Figure 3b),[44] which is defined as the blocking temperature.

Alternating Current Magnetic Susceptibility Studies. Solid evidence of the likely SMM behavior of compound **1** comes from the observation of the frequency-dependent out-of-phase ac signals in the temperature range of 1.8−5.5 K in the zero applied dc field. The $\chi_M' T$ values (Figure 4) reached a plateau between 5 and 5.5 K (ca. 14.10 $cm^3 \cdot K \cdot mol^{-1}$), and are almost frequency independent, indicating that only the ground state of the molecule is populated in the zero applied static field. Such a $\chi_M' T$ value can be used to calculate the spin value of ground

(34) van Eldik, R.; Bertini, I. *Advances in Inorganic Chemistry: Relaxometry of Water−Metal Ion Interactions*; Academic Press: Orlando, FL, 2005.
(35) (a) Kahn, O. *Molecular Magnetism*; VCH: New York, 1993; p 42. (b) Hossain, M. J.; Sakiyama, H. *Inorg. Chim. Acta* **2002**, *338*, 255–259.
(36) Plater, M. J.; Foreman, M. R. J.; Coronado, E.; Gómez-García, C. J.; Slawin, A. M. Z. *J. Chem. Soc., Dalton Trans.* **1999**, 4209–4216.
(37) Carlin, R. L. *Magnetochemistry*; Springer: New York, 1983.
(38) Figgis, B. N.; Hitchman, M. A. *Ligand Field Theory and its Applications*; Wiley-VCH: New York, 2000.
(39) Wood, J. S. *Inorg. Chem.* **1968**, *7*, 852–859.
(40) Boča, R. *Coord. Chem. Rev.* **2004**, *248*, 757–815.
(41) Boča, R. *Theoretical Foundations of Molecular Magnetism*; Elsevier: Amsterdam, 1999.
(42) Sanudo, E. C.; Wernsdorfer, W.; Abbound, K. A.; Christou, G. *Inorg. Chem.* **2004**, *43*, 4137–4144.
(43) Schelter, E. J.; Prosvirin, A. V.; Dunbar, K. R. *J. Am. Chem. Soc.* **2004**, *126*, 15004–15005.
(44) In our measurements such as ZFC−FC, a settle mode, a quasi-static-state measuring process, was employed to avoid the potential temperature error. Such a mode means that all data were obtained when the temperatures was stable enough. Therefore, the phase transition or blocking temperature could be determined like that in many reports.

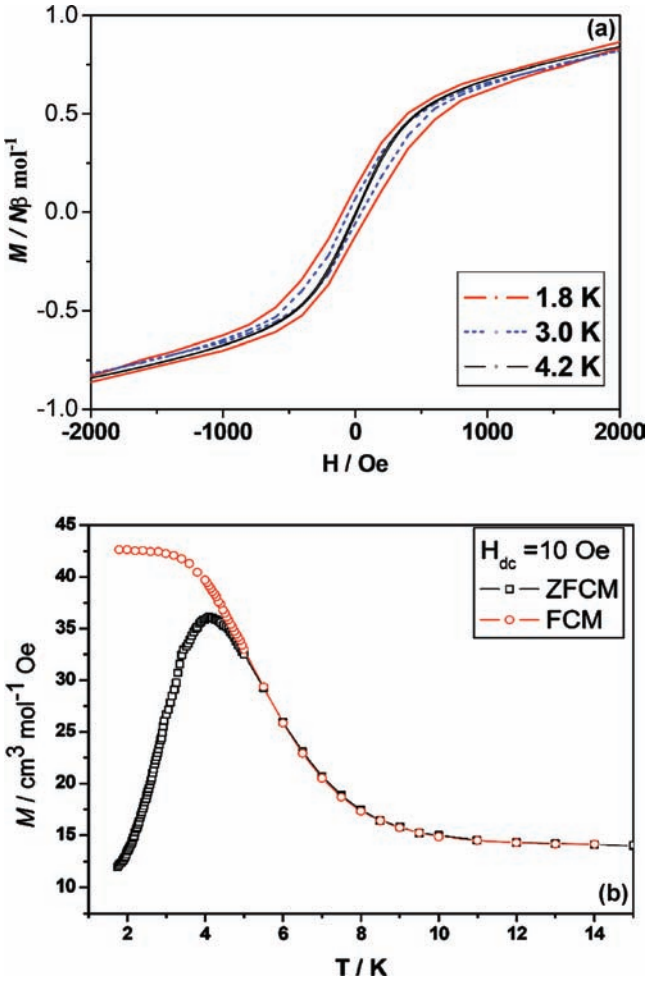

Figure 3. (a) Hysteresis loops at different temperature with the characteristic time windows of the measurements being fixed. The field increment is fixed at 0.02 T between 1.5 and −1.5 kOe. (b) ZFCM and FCM measurements in an applied field of 10 Oe with a temperature step of 0.1 K below 5 and 0.5 K in the region of 5−10 K.

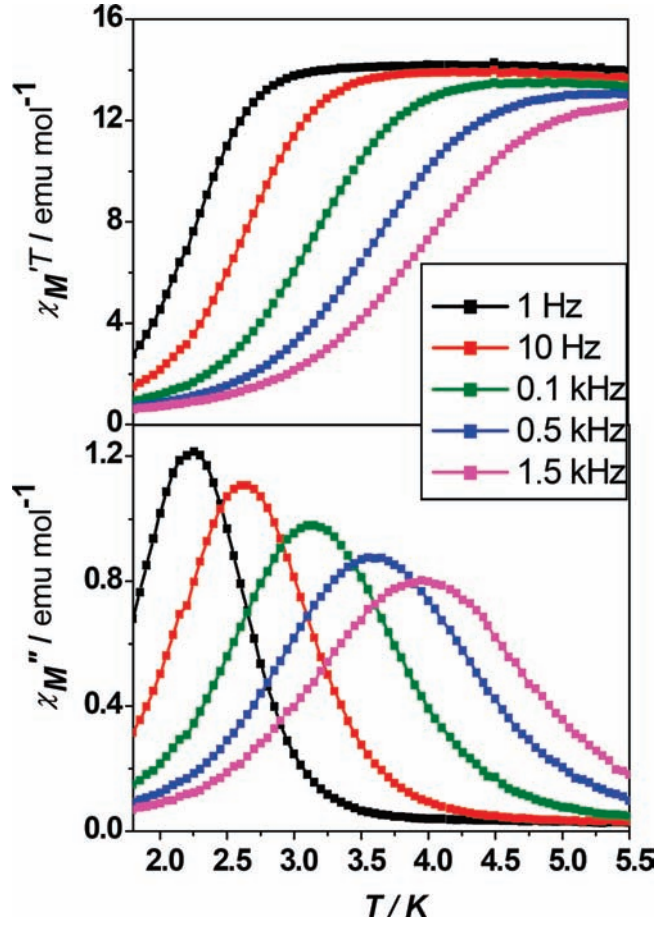

Figure 4. Temperature dependence of the in-phase (top picture) and out-of-phase (bottom picture) components of the ac susceptibilities in zero applied static field with an oscillating field of 5 Oe at frequencies of 0.1−1000 Hz. The lines are guided for view.

state, avoiding the complicated effect of the applied dc field[45,46] and the possible Zeeman effect. The value of 14.10 $cm^3 \cdot K \cdot mol^{-1}$ corresponds to an $S = 2$ state with a g' value of ca. 4.3, which is in agreement with the dc measurements in the relatively low field (100 Oe). Below 5 K, the $\chi_M'T$ values for **1** decreased rapidly, which is indicative of the onset of slow magnetic relaxation. At higher frequencies, the decrease in $\chi_M'T$ occurs at higher temperatures.

Each χ_M'' for compound **1** at a selected frequency goes through a maximum, and the maxima shift to high temperature with increasing frequency, which is the nature of superparamagnet and slow relaxing molecular clusters. The observed peaks of the out-of-phase signals correspond to the coincidence of the applied ac field oscillation frequency with the relaxation rate. Data obtained with varying frequencies of oscillation of the ac field were fitted with Arrhenius law (eq 1)

$$\tau = \tau_0 \exp(U_{eff}/k_B T) \quad (1)$$

where U_{eff} is an energy barrier for the reversal of the direction of the magnetic moment.[47,48] The best set of the obtained parameters is $U_{eff}/k_B = 38.8(5)$ K (27.0 cm^{-1}) and $\tau_0 = 5.4(3) \times 10^{-9}$ s (Figure 5), which is consistent with those in the typical SMMs, suggesting a thermally activated mechanism.

More detailed ac magnetic susceptibility experiments were carried out on compound **1**. Magnetization relaxation data were collected while the temperature of the microcrystalline sample of compound **1** was held constant and the frequencies of the ac magnetic field in dc field were varied. At a fixed temperature, the in-phase (χ_M') and the out-of-phase (χ_M'') components of the ac magnetic susceptibility were measured as the frequencies (ω) of the ac field (5 Oe amplitude) were varied from 0.01 to 1500 Hz (Figure 6). The measured plots of χ'_M versus frequency and χ''_M versus frequency for a polycrystalline powder sample of compound **1** at 3 K were fitted to a distribution of single relaxation processes and a single relaxation process, respectively.[49,50] The dashed lines result from least-squares fitting of the data to a single relaxation

(45) Chakov, N. E.; Lee, S.-C.; Harter, A. G.; Kuhns, P. L.; Reyes, A. P.; Hill, S. O.; Dalal, N. S.; Wernsdorfer, W.; Abboud, K. A.; Christou, G. *J. Am. Chem. Soc.* **2006**, *128*, 6975–6989.
(46) Chakov, N. E.; Soler, M.; Wernsdorfer, W.; Abboud, K. A.; Christou, G. *Inorg. Chem.* **2005**, *44*, 5304–5321.
(47) Sessoli, R.; Gatteschi, D.; Caneschi, A.; Novak, M. A. *Nature.* **1993**, *365*, 141–143.
(48) Sangregorio, C.; Ohm, T.; Paulsen, C.; Sessoli, R.; Gatteschi, D. *Phys. Rev. Lett.* **1997**, *78*, 4645–4648.

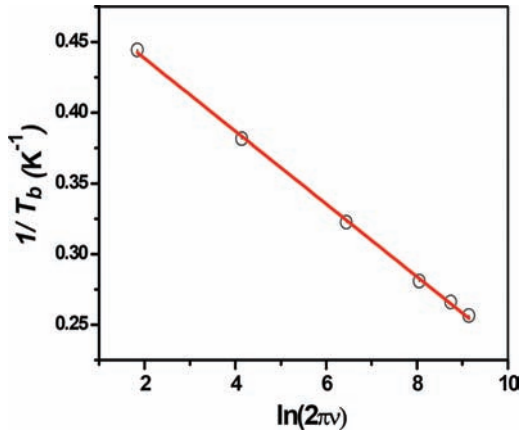

Figure 5. Plot of relaxation rate versus reciprocal temperature in zero applied static field in the range from 1 to 1500 Hz oscillating frequency. The data solid line represents the least-squares fitting of the experimental data to eq 1.

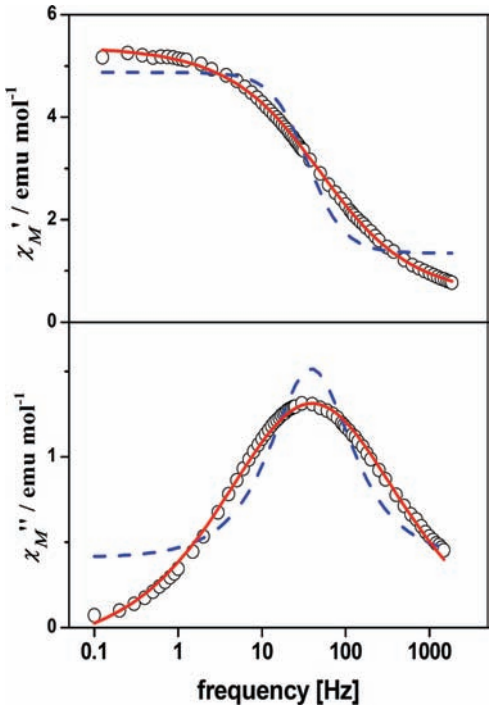

Figure 6. Plots of (top) χ_M' versus frequency and (bottom) χ_M'' versus frequency at 3.0 K in zero applied dc field for compound **1**. The blue dashed lines are least-squares fittings of the data to a single relaxation process; the red solid lines are least-squares fittings of the data to a distribution of single relaxation processes.

process, as described by eqs 2 and 3, giving $\chi_S = 1.34$ cm^3·mol^{-1}, $\chi_T = 4.87$ cm^3·mol^{-1}, and $\tau = 4.12 \times 10^{-3}$ s.

$$\chi'(\omega) = \chi_S + \frac{(\chi_T - \chi_S)}{1 + \omega^2\tau^2} \quad (2)$$

$$\chi''(\omega) = \frac{(\chi_T - \chi_S)\omega\tau}{1 + \omega^2\tau^2} \quad (3)$$

Here χ_S is the adiabatic susceptibility, χ_T is the isothermal susceptibility, $\omega = 2\pi\nu$ is the angular frequency, and τ is

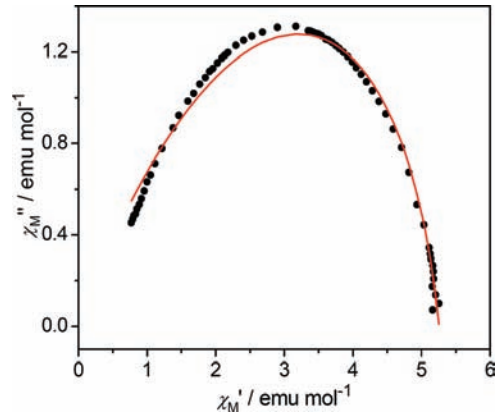

Figure 7. Cole−Cole plot of χ_M'' versus χ_M' at 3.0 K in zero applied dc field for compound **1**. The red solid line represents a least-squares fitting of the data to a distribution of single relaxation processes.

the magnetization relaxation time. Considerably improved fits are obtained when the data are fitted to a distribution of single relaxation processes, as described in eqs 4 and 5

$$\chi'(\omega) = \chi_S + \frac{(\chi_T - \chi_S)\left[1 + (\omega\tau)^{1-\alpha}\sin\frac{1}{2}\pi\alpha\right]}{1 + 2(\omega\tau)^{1-\alpha}\sin\frac{1}{2}\pi\alpha + (\omega\tau)^{2(1-\alpha)}} \quad (4)$$

$$\chi''(\omega) = \frac{(\chi_T - \chi_S)(\omega\tau)^{1-\alpha}\cos\frac{1}{2}\pi\alpha}{1 + 2(\omega\tau)^{1-\alpha}\sin\frac{1}{2}\pi\alpha + (\omega\tau)^{2(1-\alpha)}} \quad (5)$$

This gives the parameters of $\chi_S = 0.48$ cm^3·mol^{-1}, $\chi_T = 5.38$ cm^3·mol^{-1}, $\alpha = 0.38$, and $\tau = 4.03 \times 10^{-3}$ s. The resulting relaxation times (τ) obtained at a given temperature from these two fitting schemes are very similar. The main difference in fitting parameters occurs in the values of χ_S and χ_T. The data for compound **1** are also presented in Figure 7 as a Cole−Cole or Argand plot of χ_M'' versus χ_M', which gives information on the number of distinct relaxation processes that are occurring. The fitting of the data to a distribution of single relaxation processes is substantially better than that to a single relaxation process. From these data, it can be confidently concluded that only a distribution of single relaxation processes dominates the behavior of compound **1**. This magnetic behavior is reminiscent of that observed in previously reported SMMs, where the energy barrier is originated from the magnetic anisotropy.[51]

Conclusions

In summary, a new tetranuclear cobalt(II) molecular square was designed and achieved via self-assembly. The overall intramolecular ferromagnetic coupling within the low-temperature range results in a large ground state and a slow relaxation process at static zero field. It is notable that the special bridging mode of the ligand as well as the nature of Co^{II} centers plays important roles in the SMM behavior of

(49) Aubin, S. M.; Sun, Z.; Pardi, L.; Krzysteck, J.; Folting, K.; Brunel, L.-J.; Rheingold, A. L.; Christou, G.; Hendrickson, D. N. *Inorg. Chem.* **1999**, *38*, 5329–5340.

(50) Boskovic, C.; Brechin, E. K.; Streib, W. E.; Folting, K.; Bollinger, J. C.; Hendrickson, D. N.; Christou, G. *J. Am. Chem. Soc.* **2002**, *124*, 3725–3736.

(51) Sessoli, R.; Gatteschi, D. *Angew. Chem., Int. Ed.* **2003**, *42*, 268–297.

this molecule, which opens a door for exploiting new families of cobalt-based SMMs.[52]

Acknowledgment. This work is supported by the National Natural Science Foundation of China and the Natural Science Foundation of Jiangsu Province. We thank Professor Jeffrey. R. Long and Dr. H. J. Choi from the University of California, Berkeley for helpful discussions. We also thank Ms. Wei-Jie Hua and Professor Shu-Hua Li (Nanjing University) for their efforts in magnetic data fitting.

(52) Aromí, G.; Brechin, E. K. *Struct. Bonding (Berlin, Ger.)* **2006**, *122*, 1–32.

Supporting Information Available: Crystallographic information files (CIF) and XRD pattern of compound **1**. This material is available free of charge via the Internet at http://pubs.acs.org.

IC8012188